



A comparative study of structural parameters of a RCC T-girder bridge using loading pattern from different codes

Sulav Sigdel^{1,*}

¹Department of Civil Engineering, Pulchowk Campus, Institute of Engineering, Tribhuvan University, Nepal

*Corresponding email: 072bce171.sulav@pcampus.edu.np

Received: December 24, 2020; Revised: February 18, 2021; Accepted: March 06, 2021

Abstract

Nepal is an under-developed country; it is on the threshold of becoming a developing country. With new highways and railroad projects launching, construction of bridges is likely to increase. Bridges improve connectivity across the country and provide support to the country's overall economic growth. While designing a bridge, concrete properties, reinforcement properties, superstructure and substructure sections, traffic movements and loading conditions are specified. Bridges in Nepal are designed based on criteria enumerated by Indian Road Congress (IRC) code provisions. But, there are different bridge design codes used by different countries. Although these provisions follow the same basic principles, they may yield different results. The study on various structural parameters' variation is significant while selecting the code provision for the design and analysis of the bridge. In this study, a T-Girder Bridge is considered and is modelled and analyzed by vehicular loading patterns from IRC Codal Provision, AASHTO Codal Provision, and Chinese Codal Provision. This study uses CSiBridge computer software to perform the analysis.

Keywords: AASHTO loadings, Chinese loadings, IRC loadings, modelling, structural parameters, T-girder bridge

1. Introduction

The bridge's structural design consists of understanding structural members' behavior subjected to forces and loads and designing them with economy and elegance to give safe, serviceable, and durable bridge structures. The structural design of bridges of any country relies on specific codes of practices that provide essential data and standards in analyzing and designing the bridge for safe, economic and required strength criteria. The code of practices depends upon many factors such as desirable strength, economical value, environmental impacts, topological factors, soil types, seismic zones and hydrological characteristics. Till date, Nepal do not have its own code of practices for bridge design. All permanent road bridges in Nepal shall be designed as per IRC loadings or AASTHO loadings. Hence it is requisite to do thorough analysis of the results obtained from different codes before selecting the suitable code of practice. This can be done either

by manual method where bridge responses of bridge are computed manually following the code of practices. Another way is to model the bridge in the software. For this study, modeling approach is adopted and IRC loading standards for bridge, AASTHO specifications for bridge and Chinese loading are contemplated. For carriageway width less than 5.3m, IRC: 6-2010 recommends use of IRC Class A loading [Clause 204.3, Table 2]. AASTHO suggests HS_n-44 truck loading for rural and permanent bridges. This loading is practiced in Nepal. For Chinese loading, Chinese JTG Truck is selected as it is recommended by JTG D60-2015 and Yan Dai (2016).

CSiBridge Software is developed by Computers and Structures Inc., an American based company. Using CSiBridge, users can easily define bridge geometries, boundary conditions, dead and live load cases. The software creates a spine, shell, or solid objects models transformed into a mathematical finite element model. The software allows a user to perform static and dynamic analysis, linear and non-linear analysis, segmental lane analysis, default analysis and parameters analysis. The software provides a way for approximate bridge modelling with provisions of layout lines, spans, abutments, piers, pier caps, slab decks, diaphragm, and load cases (vehicle load, moving load, parapet load, material load, wearing course load, wind loads, seismic loads, hydrological loads, hydrodynamic loads, friction loads, braking loads, collision loads, and others).

Software modelling permits us to specify the structure or behavior of a system which can be used efficiently for modelling and analysis of RC T-Girder Bridge. A study conducted in STAAD Pro concludes IRC A Class loading is the most economical and optimum loading for the bridge's design compared to AASTHO specifications and Euro codes. Another research paper entitled Comparative Study of the Analysis and Design of T-Beam Girder and Box Girder Super Structure concludes that the T-beam girder is economical than the box girder. In essence, software analysis can be used effectively and efficiently for modelling and analysis of bridge structure.

The influence line is the function that provides the variation of a structural parameter at a specific point on a beam caused by a unit load moving across the beam. This function depends upon structural properties and support conditions and is different for each location and load effect. Influence lines are calculated in the software by matrix method which calculates it on the basis of known weights of a truck. This study uses dynamic moving load, and hence influence lines for each of the moving load shall be used to obtain bridge responses. This software generates influence lines for each case of moving load, and uses it to draw maximum envelopes curves.

To the best of the author's knowledge, a comparative study of RCC T-Girder Bridge's structural parameters using loading pattern of bridge design codes as per AASTHO specifications, Chinese loading, and IRC loading is not reported in the existing literature.

2. Methodology

The research methodology involves designing and analyzing an RCC T-Girder Bridge. This study adopts following processes.

1. Preliminary design of the superstructure of the bridge are performed. This includes fixing bridge span length, carriageway width, deck width, depth of deck, number of longitudinal girders, section of cross girder, number of cross girder and railing posts. These properties are provided as inputs to the software.
2. The self-weight load of different members of the bridge superstructure are calculated. Under this section, self-weight load of wearing course, curb and railing posts and their acting locations on the bridge are obtained. These loads are provided as inputs to the software.

3. The bridge model is analyzed using CSiBridge v22.1.0 software to obtain maximum and minimum envelopes of bridge responses: axial forces, shear forces, bending moments, vertical displacements, and longitudinal displacements under dead loads and vehicular loading pattern of AASTHO, Chinese, and IRC code of practices.
4. Bridge responses are compared for three code of practices.

3. Dimensioning and Modelling

3.1 Preliminary Dimension of Super Structure

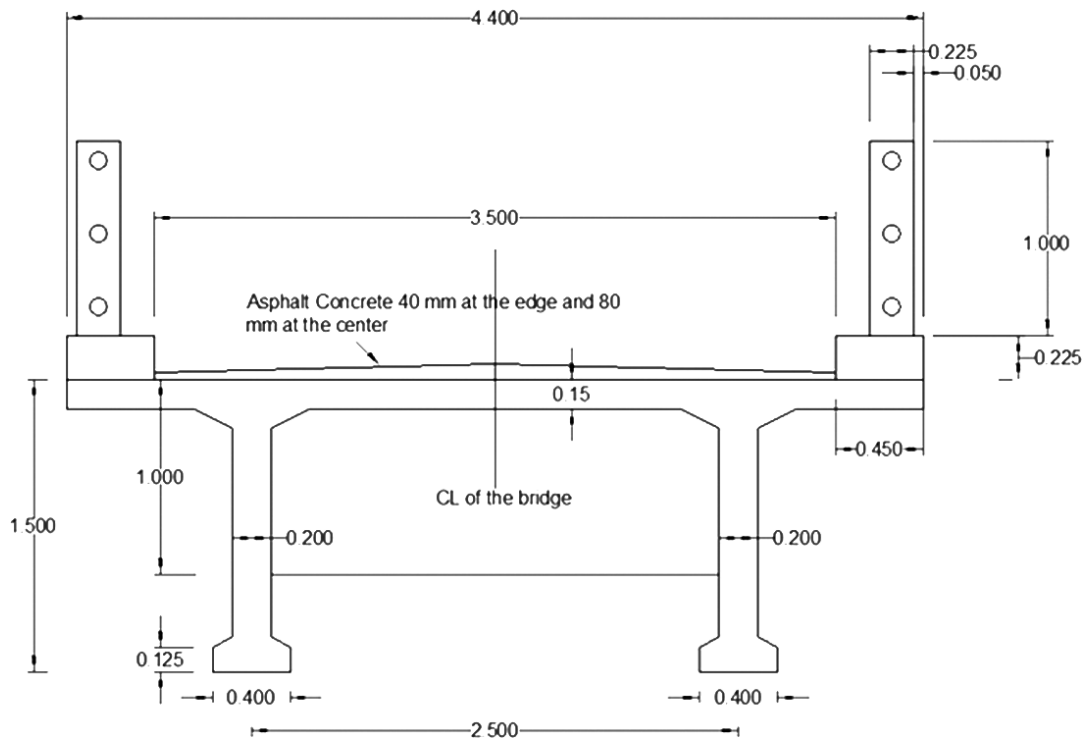
The aim of the model is to simulate dynamic truck loading passing over a bridge considering properties of model and realistic conditions. For the modelling, the bridge length is fixed considering the maximum value of linear waterway width and cross-section of the river at the bridge site. Linear waterway width is calculated following a detailed hydrological analysis of the river at the bridge site. The hydrological analysis includes the rational method, slope-velocity method, and empirical method. For a single lane carriageway, Nepal Road Standard (NRS-2070) guides the width of the carriageway, and then the width of the deck is calculated, providing curbs on both sides of the deck. Depth of deck is fixed using allowable span to depth ratio for T Girder, which satisfies serviceability condition of the girder. The thickness of the main girder and cross girder is fixed following IRC codes. The thickness of the bulb of the main girder and that of cross girder is also selected similarly.

The preliminary dimensions of superstructures are presented in Table 1.

Table 1: Preliminary Dimensions

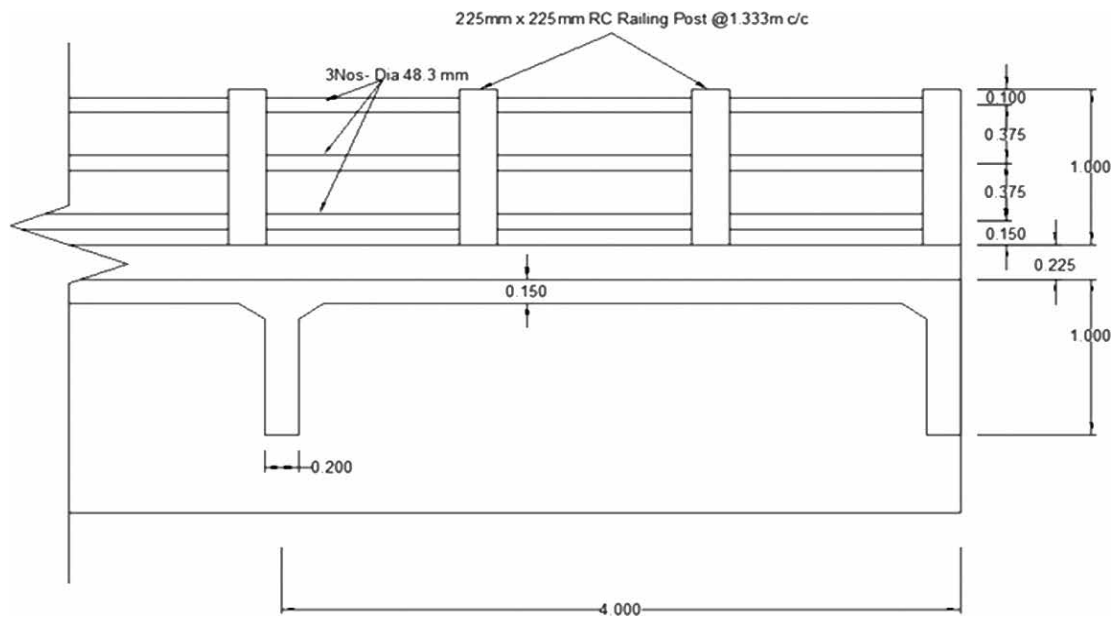
Bridge member	Data Provided
Span Length	20m
Number of Spans	1
Type of Lane	Single
Width of the Deck	4.4m
Spacing between Main Girders	2.5m
Number of Cross Girders per Span	6
Grade of Concrete	M25
Grade of Reinforcement	HYSD500
Dimension of Railing Post	1m x 225mm x 225mm
Spacing of Railing Post	1.333m c/c
Depth of Cross Girder	1m
Thickness of Cross Girder	0.2m
Wearing Course	Asphalt Concrete
Thickness of Wearing Course at the edge	40mm
Thickness of Wearing Course at the Centre of the bridge	80mm
Modulus of Elasticity of Concrete	$5000\sqrt{25} = 25000$ Mpa
Poisson's Ratio	0.2

Fig. 1 shows bridge cross section. Fig. 2 shows bridge longitudinal section, along with cross girders.



all dimensions are in meters.

Figure 1: Bridge deck section



all dimensions are in meters

Figure 2: Bridge cross girder and railings

3.2 Modeling

Modelling of the bridge is done in CSiBridge v22.1.0 software. Modelling involves creating a bridge window, adding a layout line and defining bridge component. Layout line is the first step to define a bridge object i.e., line object, and lanes. A layout line of end station at 20m is selected. The inputs for the analysis are dead loads from super-structure, material types, deck section and dynamic vehicular loads from each of the three codes. The supports of the bridge are considered as simply supported. The particular bridge input properties values are: deck section (Fig. 1), cross beam (Fig. 2), 2.64 KN/m² area load of wearing course (Fig. 3a), 2.3 KN point load of railing posts spaced at 1.33m center to center (Fig. 3b), 2.53 KN/m line load of curb (Fig. 3c) which acts through the center of gravity of curb at a distance of 0.225m from the edge of the deck, and live loads (Fig. 4, Fig. 5, and Fig. 6).

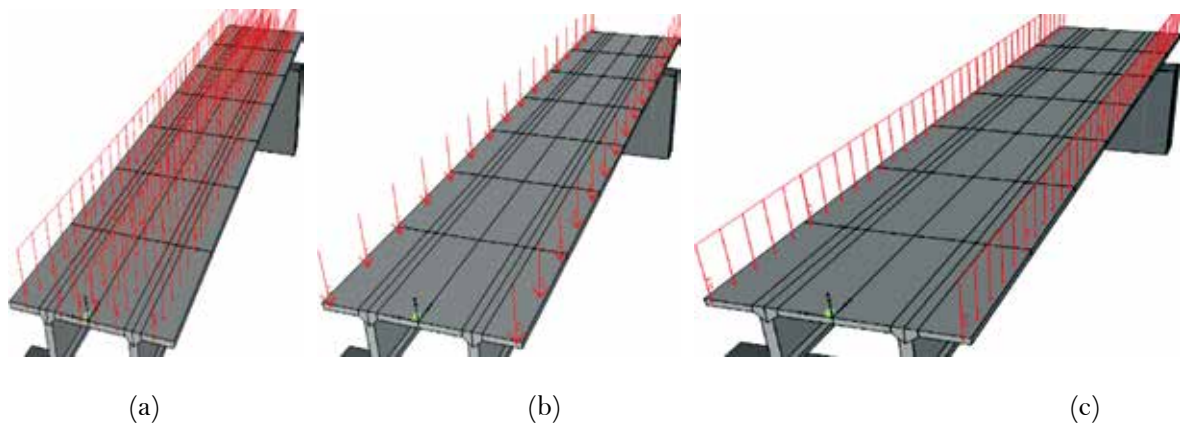


Figure 3: Dead loads in super-structure: (a) area load of wearing course, (b) point load of railing post, (c) line load of curb

The structural model is updated as an area model with a preferred maximum sub-mesh size of 2.5 units. Load discretization is at every 0.05 seconds and the output time step size is 0.05 seconds. The speed of vehicular loading is 30 KMPH. Analysis type is linear, and the time history type is direct integration. Damping and vibrations are not considered. Lateral loads are not applied externally but after modelling, lateral loads are developed. This is due to the formation of frictional forces between vehicle tire and bridge surface. Hydrodynamic loads, brake loads, wind loads and accidental loads are not used.

Live load defined in IRC code as IRC Class A (Fig. 4), in AASTHO code as HS_n-44 (Fig. 5), and in Chinese code as Chinese Truck JTG 2015 (Fig. 6) are added.

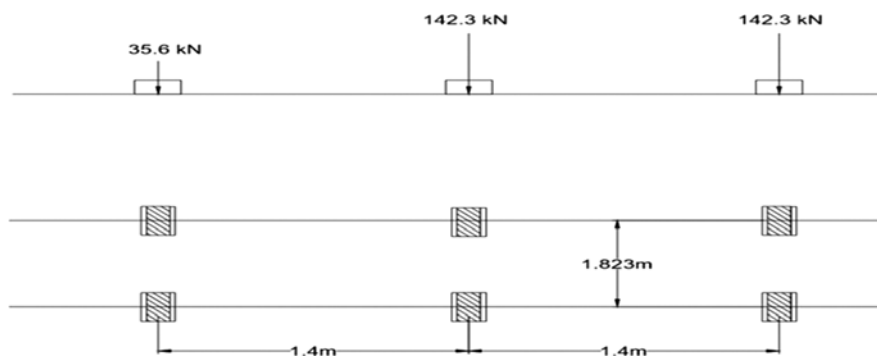


Figure 4: IRC A loading

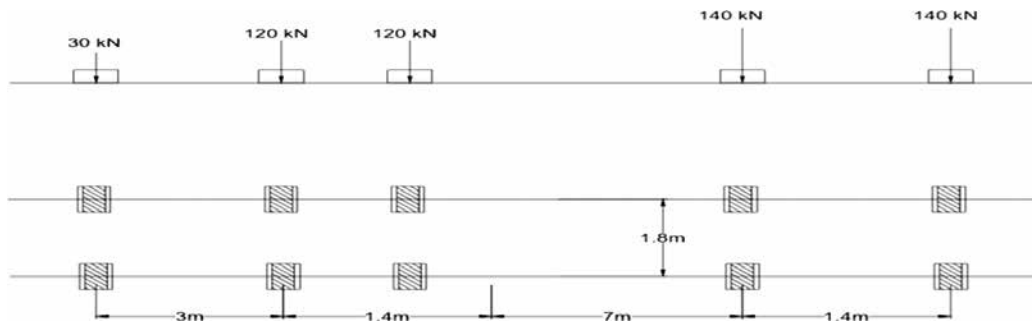


Figure 5: AASTHO HSn-44 loading

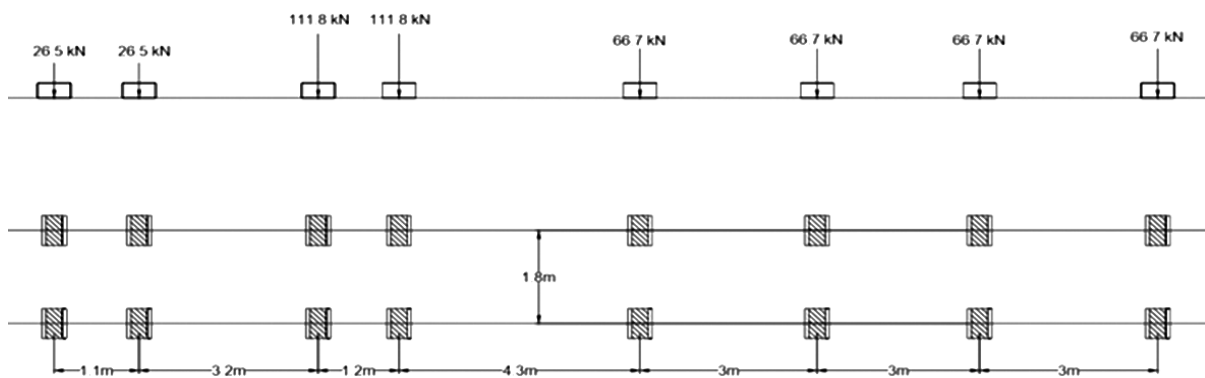


Figure 6: Chinese truck JTG loading

From Fig. 4, Fig. 5, and Fig. 6, it can be seen that total vehicular load and length of vehicular loading of IRC Class loading, AASTHO HSn-44 loading and Chinese Truck JTG loading are 320.2 KN and 2.8m, 550 KN and 12.8m, and 543.4 KN and 18.8m respectively. Length of vehicular loading has effect on influence line diagram and vehicular load impacts the value of bridge responses. Since AASTHO HSn-44 loading and Chinese Truck JTG loading have comparable vehicular loadings which are greater than IRC Class A loading, maximum bridge responses can be developed due to these two vehicular loadings. The length of vehicular loading of Chinese loading is greater than the other two. Hence it can be predicted that the maximum bridge response may be developed by Chinese loading.

The output of the dynamic vehicle-bridge simulation are the bridge responses: axial forces, shear forces, bending moments, vertical displacements, and longitudinal displacements. 3D model of the bridge before the analysis is shown in Fig. 7(a) and Fig. 7(b). The deformed model of the bridge obtained after the analysis is presented in Fig. 8.

Fig. 9 shows the deformed model of the bridge under AASTHO HSn-44 loading after 1.4 seconds of the application of truck load.

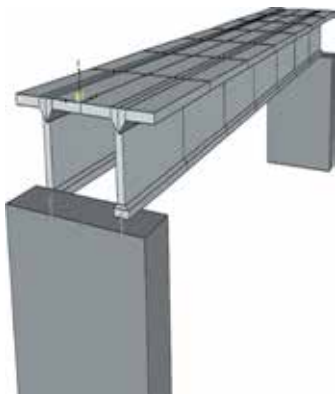


Figure 7(a): 3D model of bridge

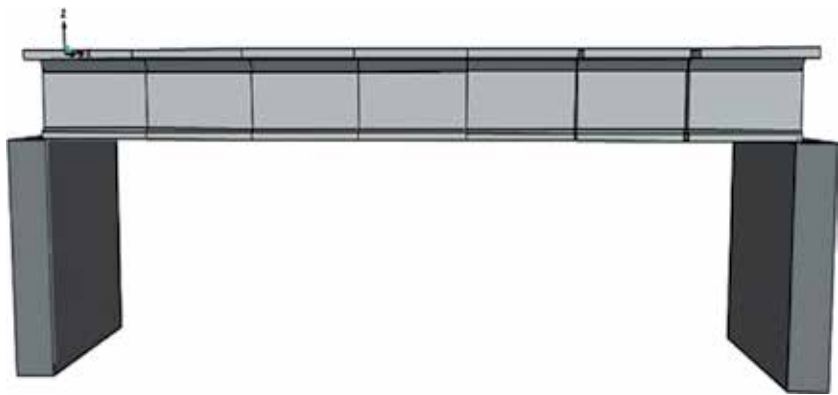


Figure 7(b): L-Section of bridge model

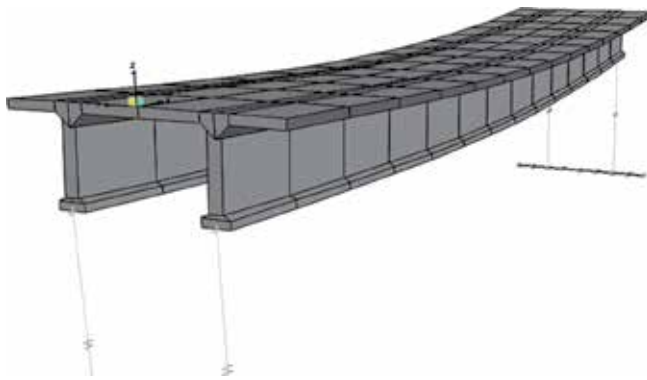


Figure 8: Bridge model after analysis

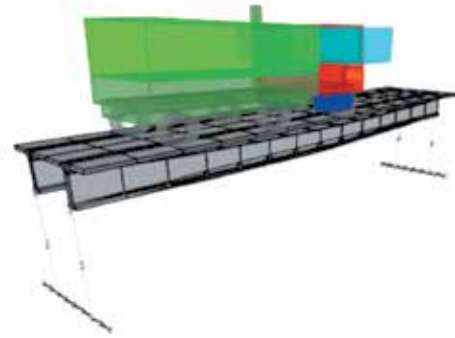


Figure 9: AASTHO Hsn-44 loading

4. Results and Discussions

Bridge object response of the deck to the combination of dead load and live load along the span of the bridge is shown in the following table (Table 2) and figures.

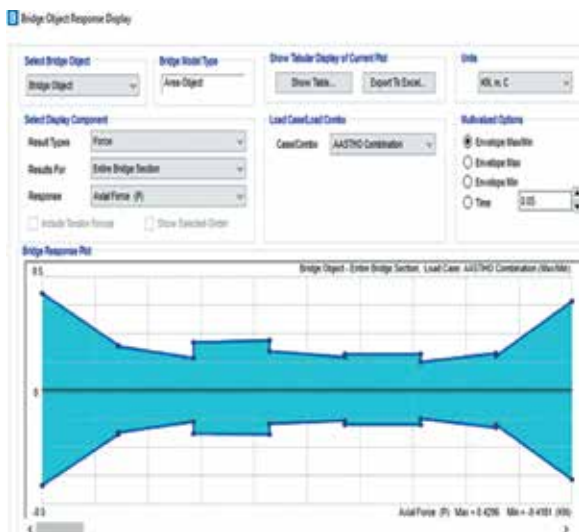


Figure 10: Axial force envelope (Hsn-44)

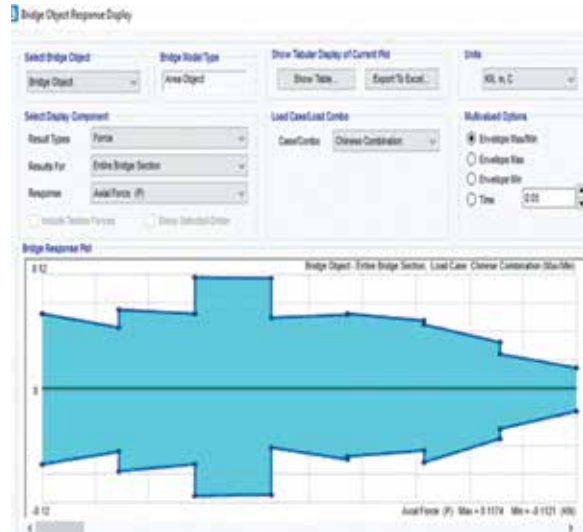


Figure 11: Axial force envelope (Chinese Truck)

Table 2: Bridge object response

Reactions		HSn-44 (AASTHO)	Truck JTG(Chinese)	Class A (IRC)
Axial Force (KN)	Max Value	0.423 (Right)	0.117 (Right)	0.145 (Right)
	Distance	0.000	5.714	0.000
	Min Value	0.122 (Left)	0.023 (Right)	0.052 (Right)
	Distance	14.286	20.000	0.000
Shear Force (KN)	Max Value	795.088 (Up)	887.122 (Up)	842.429 (Down)
	Distance	0.000	0.000	20.000
	Min Value	87.930 (Down)	85.958 (Down)	89.974 (Up)
	Distance	11.429	11.429	8.571
Bending Moment (KN m)	Max Value	4048.189 (CW)	4454.947 (CW)	4338.307 (CW)
	Distance	0.000	0.000	20.000
	Min Value	8.571	8.571	11.429
	Distance	1.0509 (CW)	0.1751 (CCW)	0.3195 (CW)
Vertical Displacement (mm)	Distance	20.000	20.000	20.000
	Max Value	21.840 (Down)	24.378 (Down)	23.271 (Down)
	Distance	11.429	11.429	11.429
	Min Value	0.160 (Down)	0.175 (Down)	0.156 (Down)
Longitudinal Displacement (mm)	Distance	0	20	0
	Max Value	1.304 (Left)	1.470 (Left)	1.395 (Left)
	Distance	20	0	20
	Min Value	0.299 (Left)	0.312	0.308 (Right)
	Distance	11.429	11.429	8.571

Due to dead loads and live loads on the longitudinal girder, the axial force envelopes are presented (Fig. 10, Fig. 11, and Fig. 12). The analysis shows longitudinal girder produced maximum axial force due to AASTHO combination loading at the start of the span (Fig. 10) but near mid-span, the longitudinal girder had more axial force due to the Chinese truck combination loading (Fig. 11). For IRC combination loading (Fig. 12), the longitudinal girder produced more axial force at the start of the span. Among these three loadings, AASTHO combination loading had a maximum axial force on the longitudinal girder.

Shear force envelopes are presented (Fig. 13, Fig. 14, and Fig. 15). The analysis shows longitudinal girder produced maximum shear force due to AASTHO combination loading at the start of the span (Fig. 13) and minimum shear force at a distance of 11.429 meters. Due to Chinese combination loading (Fig. 14), the longitudinal girder produced more shear force at the start of the span and minimum shear force at a distance of 11.429 meters. Due to IRC combination loading (Fig. 15), the longitudinal girder produced more shear force at the start of the span and minimum shear force at a distance of 8.571 meters. Among these three loadings, Chinese combination loading produced maximum shear force on the longitudinal girder.

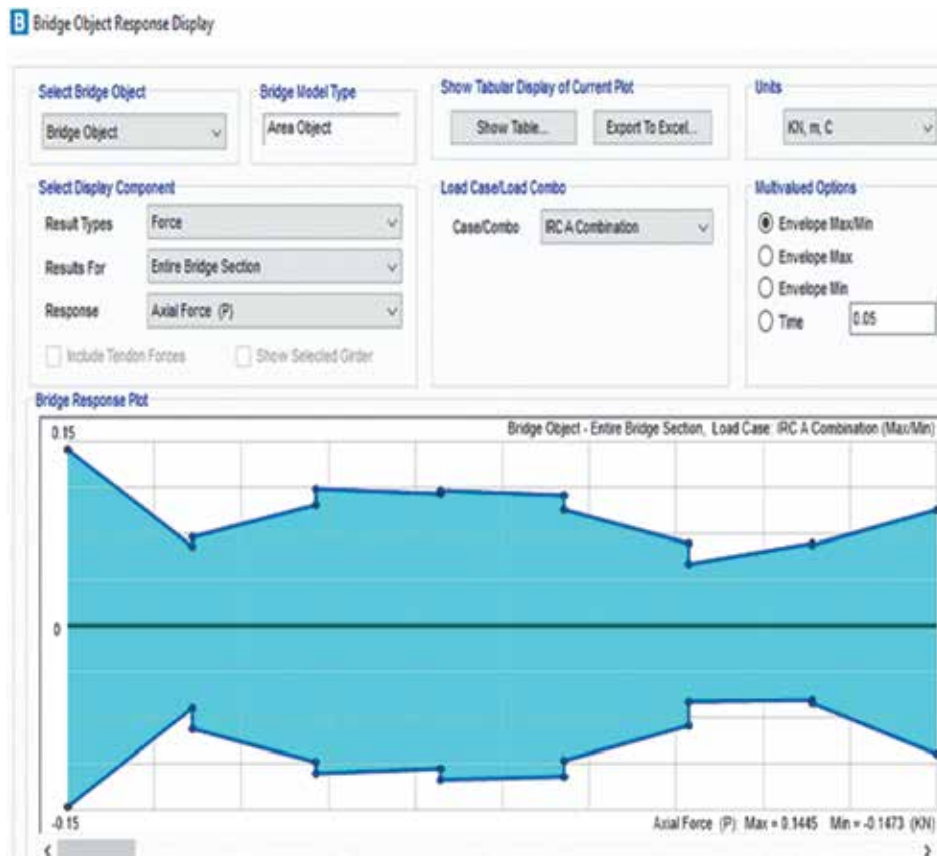


Figure 12: Axial force envelope (IRC A)



Figure 13: Shear force envelope (HSn-44)



Figure 14: Shear force envelope (Chinese Truck)

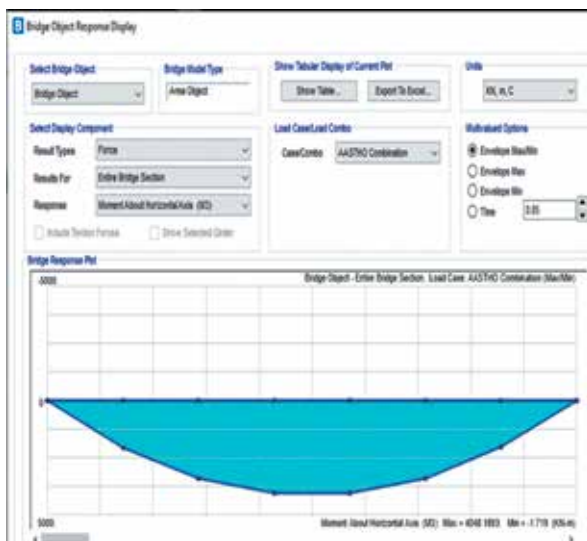


Figure 15: Shear force envelope (IRC A)



Figure 16: B.M. envelope (HSn-44)

Bending moment envelopes are presented (Fig. 16, Fig. 17, and Fig. 18). The analysis shows longitudinal girder produced maximum bending moment due to AASTHO combination loading at a distance of 8.571 meters (Fig. 16) and minimum bending moment at the end of the span (Fig.16). Due to Chinese combination loading (Fig.17), the longitudinal girder produced maximum bending moment at a distance of 8.571 meters and minimum bending moment at the end of the span. Due to IRC combination loading (Fig. 18), the longitudinal girder produced maximum bending moment at the start of the span and minimum bending moment at a distance of 8.571 meters. Among these three loadings, Chinese combination loading produced maximum bending moment on the longitudinal girder.

Vertical displacement due to dead loads and live loads on longitudinal girder are shown (Fig. 19, Fig. 20, and Fig. 21). The analysis shows that longitudinal girder produced maximum vertical displacement due to AASTHO combination loading (Fig. 19) at a distance of 11.429 meters and minimum vertical displacement at the start of the span. Due to Chinese combination loading (Fig. 20), the longitudinal girder produced maximum vertical displacement at a distance of 11.429 meters and minimum vertical displacement at the end of the span. Due to IRC combination loading (Fig. 21), the longitudinal girder produced maximum vertical displacement at a distance of 11.429 meters and minimum vertical displacement at the start of the span. Among these three loadings, Chinese combination loading produced maximum vertical displacement on the longitudinal girder.

Longitudinal displacement envelopes are presented (Fig. 22, Fig. 23, and Fig. 24). The analysis shows that longitudinal girder produced maximum longitudinal displacement due to AASTHO combination loading at the end of the span (Fig. 22) and minimum longitudinal displacement at a distance of 11.429 meters. Due to Chinese combination loading (Fig. 23), the longitudinal girder produced maximum longitudinal displacement at the start of the span and minimum longitudinal displacement at a distance of 11.429 meters. Due to IRC combination loading (Fig. 24), the longitudinal girder produced maximum longitudinal displacement at the end of the span and minimum longitudinal displacement at a distance of 8.571 meters. Among these three loadings, Chinese combination loading produced maximum longitudinal displacement on the longitudinal girder.

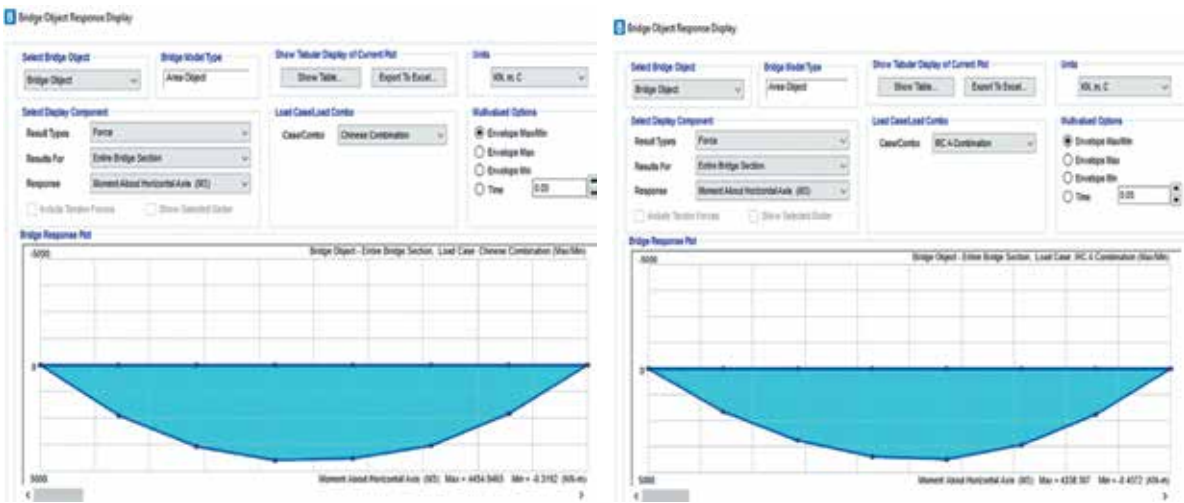


Figure 17: B.M. envelope (Chinese Truck) Figure 18: B.M. envelope (IRC A)

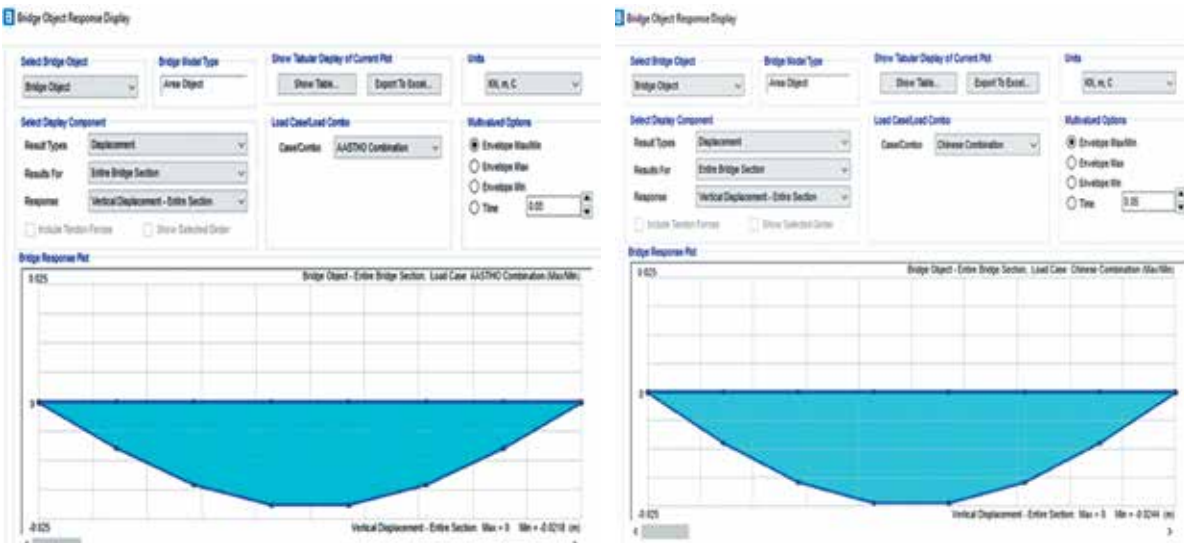


Figure 19: Vertical displacement (HS19-44)

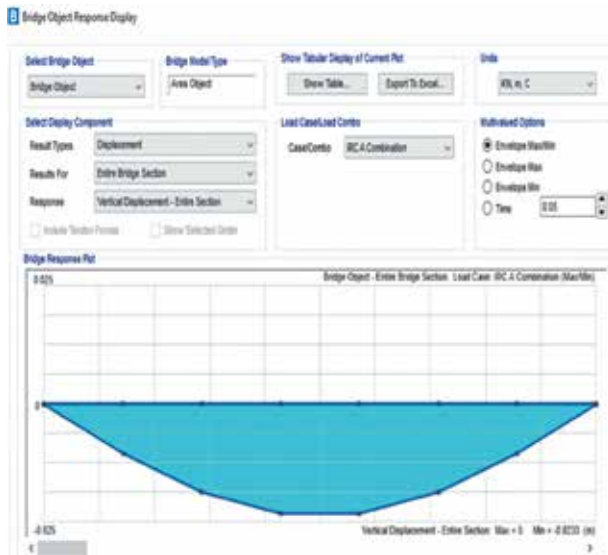
Figure 20: Vertical displacement (Chinese Truck)

From these data, it can be seen that Chinese combination provides maximum values of shear forces, bending moments, vertical displacement and longitudinal displacement. This is due to the fact that axle load and total load of Chinese JTG Truck is greater than that of IRC Class A loading and AASTHO HS19-44 loading.

5. Conclusions

Bridge design codes adopted by different countries may indicate variation in structural parameters for the design of bridges. Thus, to obtain comparative statement structural parameters, three bridge design codes are considered, and detailed modelling of the T-Girder Bridge is done in CSiBridge 2020 v21.1.0. In the design of bridge longitudinal girders with Chinese codes shear forces, bending moment, vertical displacement, and longitudinal displacement are greater (Table 2) than the other two, i.e. AASTHO specifications and IRC codes. The longitudinal girder design using IRC codes acquired axial force, shear force, bending moment, vertical displacement, and longitudinal displacement values in between the other two codes, i.e. AASTHO

specifications and Chinese codes. This depicts that IRC Class A loading provides the right balance between safety and serviceability for the design.



(HSn-44) (Chinese Truck)

Figure 21: Vertical displacement (IRC A)

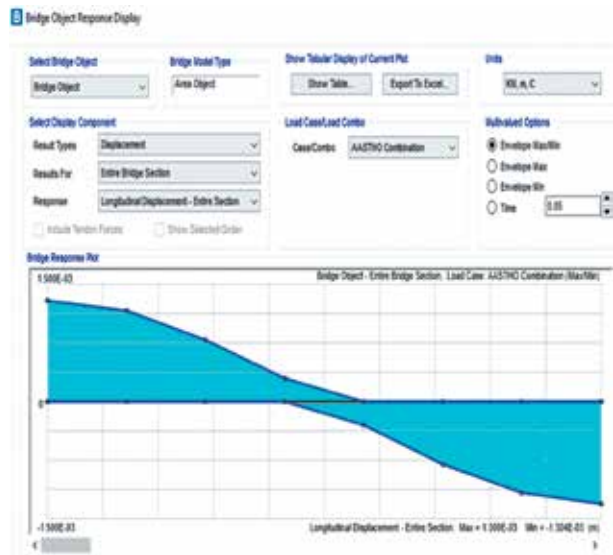
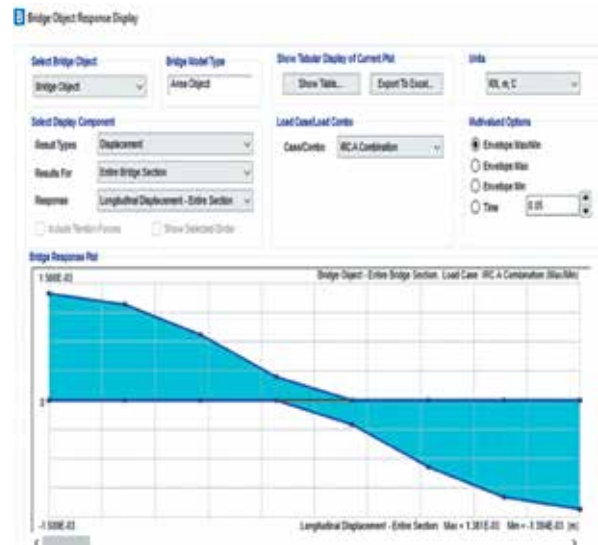


Figure 22: Longitudinal displacement (AASTHO)



Figure 23: Longitudinal displacement (Chinese)



(HSn-44)

Figure 24: Longitudinal displacement (IRC A)

(Chinese Truck) (IRC A)

This study presents the results based on three bridge design codes only. Future studies may incorporate Euro codes, Great Britain codes, Canada codes, and International design codes. Variation of steel reinforcement in main girder, cross girder, and abutment can be studied which may provide a basis for economic comparison of the bridge design codes. Since CSiBridge uses a transformed mathematical finite-element model by meshing the material domain and assigning material properties, decreasing the mesh size, reducing load discretization,

and reducing output time step size gives more accurate results. For more detailed analysis, researchers can vary the width of the deck and length of the span.

Conflict of Interests

Not declared by authors.

References

- AASHTO (2010), "AASHTO LRFD Bridge Design Specifications". American Association of State Highway and Transportation Officials, 5th Edition. Washington DC.
- Bhadauria D. S. and Patel, R. (2017), "Comparative Study of RCC Bridge for Central Zone of India for Different Sections of Girder". International Journal for Scientific Research & Development, Volume 5, and Issue 4, 2017.
- Bhat S.B. (2004), "Development of Highway Bridge loading for Nepal". Final thesis report, in the partial fulfilment of the requirements of the degree of Master of Science in Structural Engineering, IOE, Pulchowk Campus, Nepal.
- Buckland, P.G. and Sexsmith, R.G. (1980), "A comparison of design loads for highway bridges". Buckland and Taylor Ltd, North Vancouver, B.C, Canada V7P 2Y4.
- Buckle I.G. (1996), "Overview of Seismic design methods for bridges in different countries and future directions". Department of Civil Engineering and National Center for Earthquake Engineering Research, the State University of New York at Buffalo, New York, United States of America 14261.
- Chan, T.H.T., and O'Connor, C. (1990), "Wheel Loads from Highway Bridge Strains: Field Studies." Journal of Structural Engineering, ASCE, Vol. 116, No. 7.
- Chan, T.H.T., and O'Connor, C. (1990b), "Vehicle Model for Highway Bridge Impact." Journal of Structural Engineering, ASCE, Vol. 116, No. 7.
- Dai, Y. (2016), "Study on highway bridge vehicle load standard value". International Conference on Civil, Transportation and Environment (ICCTE). Shaanxi, 710065, China.
- G.B. 50011(2010), "Code for Design of Concrete Structures", National Standard of the People's Republic of China, Beijing.
- Gautam, M. (2000), "Bridge Loadings of different countries and in the context of Nepal". Final thesis report, in partial fulfilment of the requirements of the degree of Master of Science in Structural Engineering, IOE, Pulchowk Campus, Nepal.
- I.S. 456:2000, "Code of Practice for Plain and Reinforced Concrete". Bureau of Indian Standards. New Delhi, India.
- IRC 6-2010, "Standard Specifications and Code of Practice for Road Bridges". Section II, loads and stresses. The Indian Roads Congress. New Delhi, India.
- IRC: 21-2000, "Standard Specifications and Code of Practice for Road Bridges, Section III, Cement Concrete (Plain and Reinforced)". The Indian Roads Congress. New Delhi, India. 2000.
- IRC: S.P 54-2000, "Project Preparation Manual for Bridge". The Indian Roads Congress. New Delhi, India. 2000.
- JTG D60-2015, "General code for design of highway bridges and culverts[S]". People's traffic press. Beijing
- Nepal Road Standard-2070, Government of Nepal, Ministry of Physical Planning and Works, Department of Roads. 2070
- Paval, P. (2015), "Analysis of Multi-Cell Prestressed Concrete Box-Girder Bridge". International Journal of Engineering Technology Science and Research IJETS (ISSN) 2394 – 3386. Vol 3.
- Pokharel, M. (2013), "Comparative Study of RCC T-Girder Bridge with Different Codes". Final thesis report in the partial fulfilment of the Master of Science in Structural Engineering requirements. IOE, Pulchowk Campus. Lalitpur, Nepal.
- Qaqish, Fadda, and Akawwi. (2008), "Design of T-Beam Bridge by Finite Element Method and AASHTO Specification". KMITL Sci. J. Vol.8 No.1.
- Raina V. K. (2007), "Concrete Bridge practice analysis, Design, and Economics". 2nd Edition.
- Rajamoori, A.K. and Krishna, B.V. (2014), "Design of Pre-Stressed Concrete T-Beam Bridges". International Journal of Bridge Engineering (IJBE), Vol. 2, No. 3, (2014), pp. 01-14.
- Raju, N.K. (2010), "Design of Bridges". 4th edition.
- Ravi K and Jagdish Chand (2019), "Design and Analysis of Bridge Girders using Different Codes". International Journal of Engineering Research & Technology (IJERT). Vol. 8, Issue 07. (July-2019).
- Saxena, A. and Dr Maru S. (2013), "Comparative Study of the Analysis and Design o T-Beam Girder and Box Girder Super Structure". International Journal of Research in Engineering & Advanced Technology (IJREAT), Vol. 1, Issue 2,

(April-May, 2013).

Victor, D.J. (2007), "Essentials of Bridge Engineering". 6th edition.

Vijaykumar, S.P. and Mohan, K (2016), "Analysis of Bridge Girder with Beam and without Beam. International Journal of Civil Engineering and Technology, 7(5), 2016, pp.337–346.

Vishal, Gore, and Salunke. (2014), "Analysis and Design of Prestressed Concrete Girder". International Journal of Inventive Engineering and Sciences (IJIES) Volume-2, Issue-2, January 2014.

Wang, T.L. and Huang, D.Z. (1992), "Computer Modeling Analysis in Bridge Evaluation." Report No. FL/DOT/RMC/0542(2)-4108. Structural Research Centre. Department of Transportation, Tallahassee.